




## RESEARCH ARTICLE

WILEY

# How brain networks tic: Predicting tic severity through rs-fMRI dynamics in Tourette syndrome

Shukti Ramkiran<sup>1,2,3</sup>  | Tanja Veselinović<sup>1,2</sup> | Jürgen Dammers<sup>1</sup> |  
 Arnim Johannes Gaebler<sup>2,3,4</sup> | Ravichandran Rajkumar<sup>1,2,3</sup>  | N. Jon Shah<sup>1,3,5,6</sup>  |  
 Irene Neuner<sup>1,2,3</sup>

<sup>1</sup>Institute of Neuroscience and Medicine 4 (INM-4), Forschungszentrum Juelich, Juelich, Germany

<sup>2</sup>Department of Psychiatry, Psychotherapy and Psychosomatics, RWTH Aachen University, Aachen, Germany

<sup>3</sup>JARA – BRAIN – Translational Medicine, Aachen, Germany

<sup>4</sup>Institute of Physiology, Faculty of Medicine, RWTH Aachen University, Aachen, Germany

<sup>5</sup>Department of Neurology, Faculty of Medicine, RWTH Aachen University, Aachen, Germany

<sup>6</sup>Institute of Neuroscience and Medicine 11 (INM-11), JARA, Forschungszentrum Juelich, Juelich, Germany

## Correspondence

Irene Neuner, Univ.- Prof. Dr. med. Irene Neuner, Institute of Neuroscience and Medicine 4, INM-4, Forschungszentrum Juelich, Wilhelm-Johnen-Straße, 52425 Juelich, Germany.  
 Email: [i.neuner@fz-juelich.de](mailto:i.neuner@fz-juelich.de)

## Abstract

Tourette syndrome (TS) is a neuropsychiatric disorder characterized by motor and phonic tics, which several different theories, such as basal ganglia-thalamo-cortical loop dysfunction and amygdala hypersensitivity, have sought to explain. Previous research has shown dynamic changes in the brain prior to tic onset leading to tics, and this study aims to investigate the contribution of network dynamics to them. For this, we have employed three methods of functional connectivity to resting-state fMRI data – namely the static, the sliding window dynamic and the ICA based estimated dynamic; followed by an examination of the static and dynamic network topological properties. A leave-one-out (LOO-) validated regression model with LASSO regularization was used to identify the key predictors. The relevant predictors pointed to dysfunction of the primary motor cortex, the prefrontal-basal ganglia loop and amygdala-mediated visual social processing network. This is in line with a recently proposed social decision-making dysfunction hypothesis, opening new horizons in understanding tic pathophysiology.

## KEYWORDS

dynamic functional connectivity, dynamic network topology, resting state fMRI, static network topology, tic pathophysiology, visual social-processing network

## 1 | INTRODUCTION

Tourette syndrome (TS) is a complex and chronic neuropsychiatric disorder that presents itself with other comorbidities, such as attention deficit disorder (ADHD) and obsessive-compulsive disorder (OCD), in up to 90% of cases (Cavanna et al., 2009; Robertson et al., 2017). This neurodevelopmental condition is characterized by involuntary movements and vocalizations, known as tics, often present along with emotional and social disturbances (Robertson et al., 2017). There is a growing tendency to understand complex neuropsychiatric disorders

such as TS as a network problem rather than as isolated disturbances in specific brain regions (Bassett et al., 2018). For this reason, the interplay within and between large-scale brain networks through the means of functional connectivity analyses is gaining particular interest. Functional connectivity is generally defined as the ‘temporal coincidence of spatially distant neurophysiological events’ (Friston, 1994) and can be assessed at different spatial or temporal scales (Friston, 2011). Functional magnetic resonance imaging (fMRI) is frequently employed as a non-invasive tool to study functional connectivity with relatively high spatial resolution (Rogers et al., 2007). In this

This is an open access article under the terms of the [Creative Commons Attribution-NonCommercial-NoDerivs](https://creativecommons.org/licenses/by-nc-nd/4.0/) License, which permits use and distribution in any medium, provided the original work is properly cited, the use is non-commercial and no modifications or adaptations are made.

© 2023 The Authors. *Human Brain Mapping* published by Wiley Periodicals LLC.

context, functional connectivity is most commonly assessed as a 'static phenomenon' by quantifying the correlation of the entire BOLD time-series extracted from two different locations in the brain. Abnormal patterns of static functional connectivity in different brain circuits have been shown in TS (Ramkiran et al., 2019; Wen, Liu, Rekik, Wang, Chen, et al., 2017; Worbe et al., 2012), and several different theories, such as failure of network maturation (Albin & Mink, 2006), lack of inhibition (Jackson et al., 2015), basal ganglia circuits dysfunction (Ramkiran et al., 2019) and amygdala dysfunction (Neuner et al., 2010), have tried to explain the different dimensions of the disorder independently. However, several cardinal features, such as the nature of the tics, lifetime prevalence of the disorder and gender disparity, remain unexplained by these different theories. A more recent hypothesis proposes TS to be a disorder of the social decision-making network (SDM) (Albin, 2018), bringing together all the previous models and unexplained cardinal features under one umbrella. This hypothesis puts forth the idea that TS is a disorder of social communication resulting from developmental abnormalities at several levels of the SDM (Albin, 2018).

In contrast to the more commonly studied static functional connectivity, dynamic functional connectivity (DFC) refers to the analysis of functional connectivity changes over time. It is effective in capturing temporal variations in spatial connectivity, enabling the identification of different mental states at rest (Mooneyham et al., 2017). Several studies have shown this method to be useful in identifying transient states of mindfulness and mind-wandering (Mooneyham et al., 2017), and aberrant transient states in schizophrenia (Damaraju et al., 2014) and traumatic brain injury (Vergara et al., 2018).

There are multiple approaches for obtaining the DFC from fMRI data. The most common approach is the use of a sliding-window to capture connectivity in short time periods for the whole duration of the scan. This approach is useful in reliably capturing slow dynamics as the frequency is limited by temporal smoothing, that is, the length of the sliding window. Typically recommended window lengths range from 20 to 30 times the repetition time of the fMRI sequence (Hutchison et al., 2013). Another more recent approach to DFC is an estimated form of DFC as opposed to the direct sliding window approach. In this manuscript, we abbreviate the direct sliding window approach as dSW and the ICA based dynamic connectivity as dICA. The estimated connectivity in dICA is obtained via a group level ICA decomposition of static connectivity, followed by a generalized psycho-physiological interaction model (gPPI) back-projection (Alfonso Nieto-Castanon, 2020) of the identified IC networks. The gPPI back-projection estimates the connectivity at a certain timepoint as a weighted sum of the identified ICs, under the assumption that the BOLD activity of a region at the next time point depends on its current BOLD activity and its interaction with all the other regions (functional connectivity). The advantage of this approach is that it allows investigation of instantaneous connectivity at a higher signal-to-noise ratio, as noise ICs can be removed prior to back projection. The disadvantage is, however, that the connectivity is estimated and not true, and the identification of ICs depends on the dataset. In contrast, the dSW captures true connectivity directly at the individual

level, but it is limited by the minimum window length and therefore can only be used to capture slow dynamics. As patients can experience tics at any point in time, and this sudden onset of tics may be attributed to sudden network switching; it necessitates the investigation of network dynamics. The sudden onset of tics during the resting state has been monitored using a video camera system (Neuner et al., 2007), and changes in brain activation patterns from 2 s before tic onset until the actual tic onset have been shown in previous studies (Neuner et al., 2014). As both the dSW and dICA approaches provide different aspects of information on dynamics, we decided to include both approaches in our investigation.

The assessment of network topological properties of the brain allows us to understand the organization and communication strategies employed by the brain. Previous studies on TS have shown disruptions in the balance between local specialization and global integration mechanisms in whole brain-structural networks (Wen, Liu, Rekik, Wang, Zhang, et al., 2017) and defects in network maturation, reflected by losses of hub regions in resting-state cortico-basal ganglia functional networks (Worbe et al., 2012). Classical static functional networks show the overall picture of functional organization (division of roles, designation of subnetworks for specialized information processing etc.) in the brain (Achard & Bullmore, 2007; Alfonso Nieto-Castanon, 2020; Bassett & Bullmore, 2006; Bullmore & Sporns, 2009; Rubinov & Sporns, 2010; Sizemore & Bassett, 2018; Sporns, 2013; Whitfield-Gabrieli & Nieto-Castanon, 2012). However, they lack information about transients or fluctuations in network organization. To bridge this gap, there is growing interest in the temporal network organization or the dynamic graph theory approach (Sizemore & Bassett, 2018), which offers temporal equivalents of the static graph metrics. Such measures of dynamic brain network structure may reveal important insights into the pathophysiology of mental disorders and different applications (e.g., multi-layer community analysis) generated promising biomarkers of schizophrenia (Braun et al., 2016), attention deficit hyperactivity disorder (ADHD) (Yin et al., 2022), and autism (Xie et al., 2022). To the best of our knowledge, this study is the first of its kind to investigate dynamic network organization in TS.

With converging evidence showing TS as a network disorder and the need to obtain a complete picture of tic pathophysiology, the investigation of network dynamics seems to be a crucial step. Therefore, in this study, we have examined the ability of direct and indirect dynamic network metrics to predict tic severity.

## 2 | METHODS

### 2.1 | Tic severity

The gold standard for assessing the severity of tics in patients with TS and other tic disorders is the Yale global tic severity scale (YGTSS). It evaluates the number, frequency, intensity, complexity, and interference of motor and phonic symptoms (Leckman et al., 1989). It is a semi-structured interview followed by a questionnaire which results

in five different ratings: total motor tic score, total verbal tic score, total tic score (motor + verbal), overall impairment rating, which reflects the impact of tics on their daily lives and activities and a global severity score. The global score is determined by adding together the total motor, verbal and impairment scores and ranges from 0 to 100. In clinical practice, the YGTSS is used to track changes in tic behaviour or to monitor treatment outcomes (Storch et al., 2011). A recent study has shown YGTSS to be robust against the effects of comorbidities such as OCD and ADHD, making it a good choice to investigate the pathophysiology of tics independently of other comorbidities (Haas et al., 2021).

## 2.2 | Participants

Following prior informed consent, a total of 36 adult patients fulfilling the DSM-IV-TR (American Psychiatric Association, 2000) criteria for TS participated in this study. Of these, five patients additionally suffered from obsessive-compulsive disorder (OCD), and two from attention-deficit-hyperactivity disorder (ADHD), as per the DSM-IV classification. Fourteen of the patients were on medication. Tic severity was measured using the YGTSS. Subsets of subjects from this dataset focusing on other analysis strategies have been previously published in Neuner et al. (2014), Ramkiran et al. (2019) and Werner et al. (2010). Subjects with incomplete imaging or demographic data or with images corrupted by artefacts (motion, coverage, susceptibility etc.) were excluded from further analyses. After exclusion, 17 patients (12 male, 5 female, age:  $32 \pm 11$  years) were subjected to further analyses, demographic details of which can be found in Table 1. All patients had normal or corrected-to-normal vision, no hearing loss and reported a strong right-hand preference (Werner et al., 2010). The study was conducted according to the Declaration of Helsinki and under granted approval from the ethics committee of the medical faculty RWTH Aachen, Germany.

## 2.3 | Data acquisition

The image acquisition protocol comprised structural MRI, resting-state fMRI, task fMRI and diffusion MRI sessions acquired on a 1.5 T whole-body MR system (Sonata, Siemens, Germany) at the Forschungszentrum Jülich. An MR-compatible video camera system was used to monitor tics in TS patients during the scanning sessions (Neuner et al., 2007). The resting-state fMRI data were acquired using a T2\*-weighted echo-planar imaging sequence (scanning parameters: TE = 60 ms, TR = 3200 ms, flip angle =  $90^\circ$ , 30 axial slices 4 mm thick, FOV = 200 mm, in-plane resolution =  $3.125 \text{ mm} \times 3.125 \text{ mm}$ , 12 min 220 volumes, eyes closed) and structural MRI acquired using a T1-weighted gradient-echo MP-RAGE sequence (scanning parameters: TI = 1200 ms, TR = 2200 ms, TE = 3.93 ms,  $15^\circ$  flip angle, FOV =  $256 \times 256 \text{ mm}^2$ , matrix size =  $256 \times 256$ , 176 sagittal slices generated, slice thickness = 1 mm, resolution = 1 mm isotropic) were used for further investigation in this study.

**TABLE 1** Demographic data – Age, gender, medication and comorbidities of all participants.

Age	Gender	Medication	YGTSS	Comorbidities
41	F	-	33	
36	M	-	68	
21	M	10 mg ESC	40	
22	F	-	57	
45	M	200 mg TIA	59	
56	F	40 mg CIT, 400 mg CBZ	63	OCD
46	F	-	46	
46	M	-	54	
28	M	-	17	
39	M	200 mg AMS, 50 mg TIA	80	OCD
24	M	-	2	
27	M	-	63	OCD, ADHD
25	M	20 mg CIT, 200 mg TIA	66	OCD
26	M	50 mg TRIM	44	
22	F	10 mg ARI, 20 mg FLX	27	
19	M	80 mg ZPR	60	
21	M	-	62	

Abbreviations: ADHD, attention deficit hyperactivity disorder; AMS, amisulpiride; ARI, aripiprazole; CBZ, carbamazepine; CIT, citalopram; ESC, escitalopram; FLX, fluoxetine; MPH, methylphenidate; OCD, obsessive-compulsive disorder; PIM, pimozone; TIA, tiapride; TRIM, trimipramine; ZPR, ziprasidone.

## 2.4 | Data pre-processing

The data were processed using standard pre-processing pipelines in CONN v20.b (Whitfield-Gabrieli & Nieto-Castanon, 2012), based on SPM12 (Friston et al., 1994). Functional pre-processing involved the following steps: realignment and unwarp (for motion and field map correction), translation of the image centre (to the origin 0,0,0), slice-timing correction, outlier scan detection and scrubbing (using ART: artefact removal toolbox, parameters: global-signal z-value threshold: 5, subject-motion threshold: 0.9 mm), and spatial normalization to an MNI152 (2 mm) template (using SPM's unified segmentation (Ashburner & Friston, 2005), parameters: functional target resolution 2 mm) and functional smoothing (FWHM 8 mm). Pre-processing of the structural images involved the following steps: translation of the image centre (to the origin 0,0,0), segmentation and normalization into MNI-space (using SPM's unified segmentation (Ashburner & Friston, 2005), parameters: structural target resolution: 1 mm). Pre-processing was followed by nuisance regression of the following confounds: noise components of WM and CSF (aCompCor: first five principal components of time series (Whitfield-Gabrieli & Nieto-Castanon, 2012)), estimated subject-motion parameters (six realignment parameters and their first derivatives), outlier scans identified

(scrubbing) and the effect of rest (to compensate for initial magnetization transient). This was followed by temporal band-pass filtering at 0.008–0.09 Hz (to minimize the impact of physiological noise stemming from respiration and heartbeat) and linear detrending. Figure 1a outlines the pre-processing steps.

## 2.5 | Static and dynamic connectivity

All connectivity analyses were performed using CONN v20.b. For static connectivity (sFC), an ROI-based functional connectivity model (bivariate correlation) was specified in the 1st-level analysis. The model included 105 regions covering the cortex (91 regions) and sub-cortex (14 regions) provided with CONN (parcellations as per the Harvard-Oxford cortical and subcortical maximum likelihood atlases). The cerebellum was excluded from the ROIs due to coverage artefacts in the images. Normalization of correlation values was performed using Fisher's z-transformation.

For dynamic connectivity, two approaches were employed. The direct approach involved decomposing each session into 24 sliding windows of length 100 s and step size 25 s. Each window comprised 35 fMRI volumes. Following this, ROI-based functional connectivity was obtained for each sliding window in a similar way to the static connectivity approach (dSW).

The indirect dynamic connectivity, or dynamic ICA approach (dICA), is a relatively new approach that was introduced with the CONN toolbox. Here, the dynamic connectivity is estimated by first obtaining the different modulatory circuits and the rate of connectivity change between the ROIs at the group level, which are then back-projected to the individual level in a gPPI model (Alfonso Nieto-Castanon, 2020). The computation involved group-level ICA decomposition of the ROI-ROI connectivity timeseries into 20 components (selected by default in CONN), removal of ICs with spatial kurtosis  $<3$  (resulted in removal of five components), gPPI back-projection of the remaining ICs to the individual subject level followed by temporal smoothing of 10 s.

## 2.6 | Thresholding

All the connectivity matrices were then imported into MATLAB R2021a, converted to raw correlation values and binarized using an absolute threshold of 0.45 (correlation values  $>0.45$  or  $<-0.45$  were retained). The value 0.45 was chosen after evaluating the network global efficiency distributions for optimal separation between random and ordered networks (maintaining optimal small-worldness) using CONN's variable threshold explorer as, brain networks have been typically shown to be small world in nature (Bullmore & Sporns, 2012).

It is important to choose the right thresholding strategy when performing binary network analyses in order to ensure correct interpretation of the individual connections and the whole network after binarization. There are several different strategies for this, each with their own set of pros and cons (Fornito et al., 2016). Two of the most common strategies are global (or weight-based) thresholding and

density-based thresholding. Global thresholding involves retaining only those connections that are larger than a certain threshold. This lays greater emphasis on the connection strengths, making sure that only strong connections are retained, at the risk that the networks have different connections densities. Density-based thresholding does exactly the opposite, making sure all networks have the same connection density at the risk of including spurious connections. Based on this one could conclude that for applications which focus on the importance of individual connections, the global thresholding approach is better; and for those which focus on network level measures such as modularity, the latter might be more appropriate. In either case, the meaning of the connection strength and its interpretation should be clear before thresholding is applied.

Another important aspect for consideration is the direction of connectivity, that is, positive or negative as they are indicative of distinct processes. Positive functional connectivity between two regions in the brain shows that these two regions are active at the same time, indicating direct involvement in the same process, while negative connectivity reflects inhibitory or complementary interaction between two regions.

Since the aim of this paper is to focus on changes in communication of individual regions, irrespective of whether it is excitatory or inhibitory in nature, we have included both positive and negative connections. Additionally, since it is important for the individual connections to be comparable from a clinical perspective, we have chosen a global thresholding strategy (correlation-based thresholding) and retained connections that are stronger than 0.45. In addition, however, we have performed analyses using density-based (or sparsity-based) thresholding, and positive-only networks, and compared the results to those in the main paper. These results and the corresponding discussion can be found in the supplementary materials.

## 2.7 | Network statics and dynamics

Static and dynamic graph theory was applied to the binary adjacency matrices. Binary adjacency matrices can be visualized as binary graphs with ROIs as nodes and the connections between them as the edges of the graphs. An edge exists if the connectivity between them is greater than the applied threshold (in our case, correlation  $>0.45$  or  $<-0.45$ ). In this context, the following metrics were calculated:

1. *Average path length*: The path length is defined as the number of edges between two nodes (minimum number of edges for shortest path length), and the average path length (APL) of a given node is the average of the shortest path lengths between that node and all other nodes in the network. It reflects the functional integration ability and the speed of serial communication through a node (Achard & Bullmore, 2007; Sporns, 2013). The temporal equivalent of the shortest path length is called the latency or the minimum number of time points that need to pass before the information can travel from one node to the other. Thus, temporal average path length (tAPL) is the average of the latencies between that



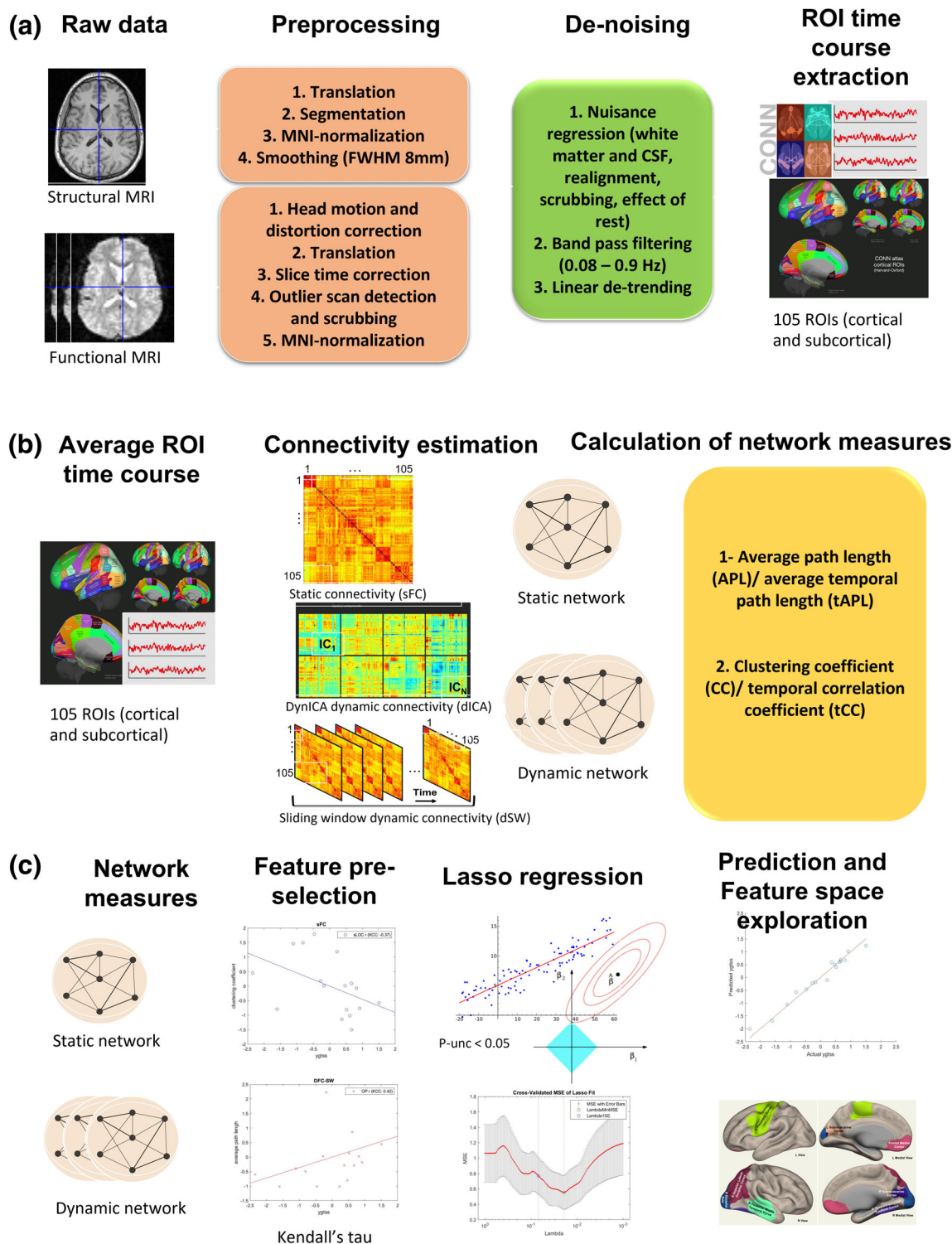


**FIGURE 1** Data processing and analysis pipeline. (a) default preprocessing and denoising pipeline using CONN; (b) Static and dynamic network analysis: calculation of static functional connectivity(sFC), dynamic ICA based dynamic functional connectivity (dICA) and sliding window dynamic connectivity (dSW) followed by application of static and dynamic graph theory; (c) feature selection and prediction: feature pre-selection using  $p\text{-unc} < 0.05$  on Kendall's tau between the YGTSS and each network measure, selected features are then fed to a leave one out (LOO-) LASSO regression model to obtain optimal parameters for the prediction of the YGTSS; finally the weights of the features in the optimal model are investigated.

node and all other nodes in the network. As before, it reflects the speed of communication in the dynamic network (Sizemore & Bassett, 2018).

2. *Clustering coefficient/temporal correlation coefficient*: Clustering coefficient (CC) is defined as the proportion of a node's neighbours that are also neighbours of each other. It is a measure of functional

segregation reflecting the extent of the specialized information processing a node is involved in. It reflects the average density and intra-connectedness of the node's subnetwork (Latora & Marchiori, 2001). Temporal correlation coefficient (tCC) is the average topological overlap of a node's neighbours between two successive time points (Sizemore & Bassett, 2018). Based on this definition, tCC reflects the stability of a node's subnetwork in dynamic performance. Nodes with a higher tCC would have a relatively stable subnetwork organization throughout the network dynamics.

## 2.8 | Feature selection and prediction

After calculation of network and node metrics for all the ROIs, the Kendall's coefficient of concordance with the YGTSS was calculated for each measure. Without correction for multiple comparisons, the measures that were significantly correlated ( $p$ -value  $< 0.05$ ) were selected as features for the YGTSS prediction model. (Table S1 lists the Kendall's tau for each measure). For this purpose, a leave-one-out (LOO) validated LASSO regression model was created, in which the network features were used as continuous independent variables. The Fisher's  $z$  transformed YGTSS was the continuous dependent variable, and gender and medication were categorical variables. LASSO regression applies a regularization term to linear regression in order to perform variable selection, thereby assigning weights to predictor variables in their order of significance and setting the weights of non-significant predictor variables to 0. Hereafter, the non-zero predictor variables identified by the model were inspected and have been discussed further. Figure 1c outlines the steps of the prediction model.

## 3 | RESULTS

### 3.1 | Connectivity estimation

The brain was divided into 105 regions of interest (ROIs) covering the cortical and subcortical areas (based on the Harvard-Oxford cortical and subcortical atlases), and the average time series of each ROI was computed. Three types of functional connectivity were computed from each ROI time series, namely:

- The static functional connectivity (sFC), which was obtained by applying a weighted GLM model (bivariate correlation with hrf weighting) to pairs of ROIs.
- The sliding window dynamic connectivity (dSW), which was obtained by temporal decomposition of the ROI time series into sliding windows of length 100 s and overlap 75 s followed by the computation of bivariate Pearson's correlation in each sliding window.
- The ICA based dynamic functional connectivity (dICA), which was obtained by group ICA decomposition of the time series of all the subjects followed by gPPI back projection of the independent components to obtain the ROI BOLD responses. The data were decomposed into 29 ICs, and temporal smoothing was applied for 10s. The number of ICs was determined by a data driven approach, using the MDL criteria in the GIFT ICA toolbox. The connectivity ICs arranged in the order of increasing kurtosis can be found in Figure 2. The top 3 ICs were removed before back-projection and dynamic functional connectivity estimation (ICs with kurtosis  $< 3$  were removed; images with low spatial kurtosis yield noise components by identifying uniformly distributed or global connectivity).

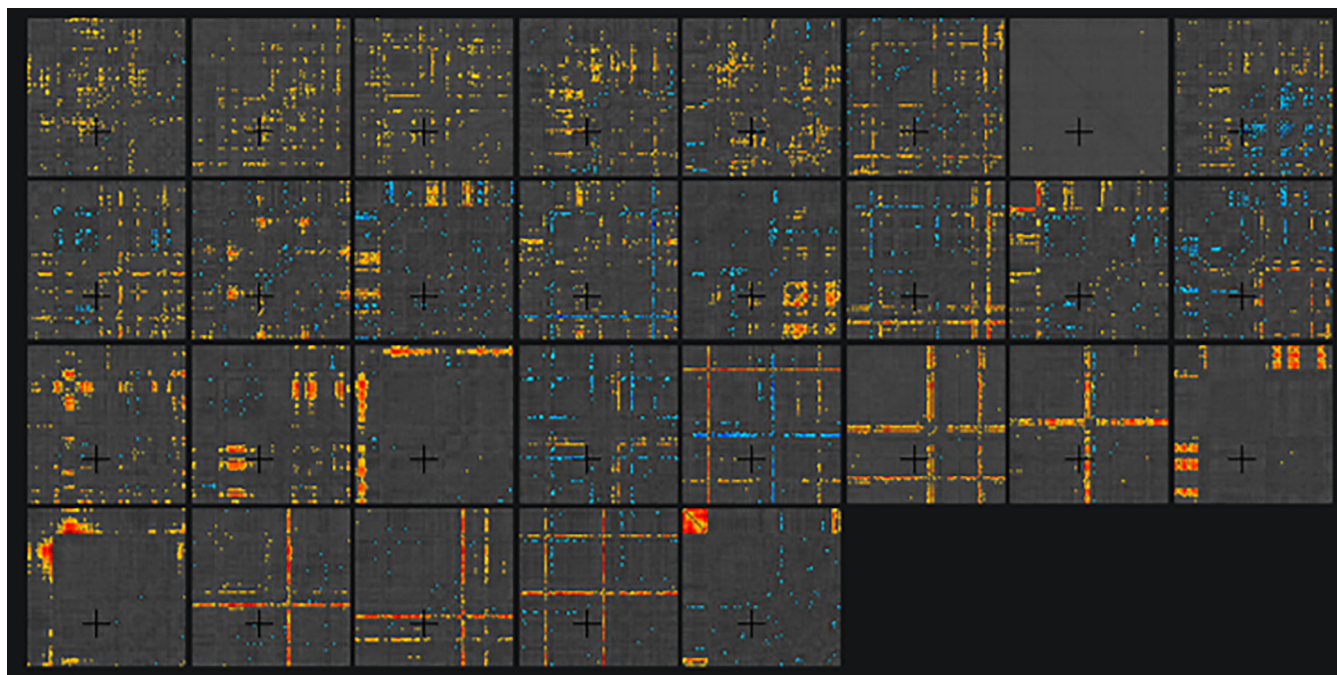


**FIGURE 2** Spatial properties of ICs obtained. The matrices are fully connected, but only connections with  $z$ -score  $> 2$  have been displayed. The first three ICs with low spatial kurtosis ( $< 3$ ) were removed before back projection and estimation of the dynamic functional connectivity.

### 3.2 | Calculation of network measures

The connectivity estimates were used to investigate network properties in the brain. Classical static network theory was applied to the static functional connectivity, and a newer dynamic network theory was applied to the dynamic functional connectivity. Both approaches used binarized adjacency matrices, and the binarization threshold was chosen as 0.45 for the correlation coefficient between two ROIs. Thus connections  $>0.45$  or  $<-0.45$  were retained as 1s and others were converted to 0s. This threshold was chosen to retain the maximum number of connections while at the same time obtaining a small world distribution (maximum separation between a random graph and a regular lattice), after inspecting the variable threshold explorer in CONN v20.b. The static network distribution, along with the comparison of regular versus a random graph for different thresholds, can be found in Figure 3a. The distribution of APL and tCC were inspected for variable thresholds applied to the dynamic networks as well (Figure 3b). Dynamic networks have also shown to be small world in nature (Tang et al., 2010). Since the inspection confirmed that 0.45 was a good threshold to maintain dynamic small-world organization, the same was used to maintain consistency. Moreover, a correlation value of 0.4 or higher can be considered clinically relevant when investigating synchrony/communication between regions. Thus, choosing a value lower than 0.4 would mean including weak and strong connections in the same network, reflecting a clinically incorrect picture. On the other hand, a value too high (such as higher than 0.5) would be significant loss of connections to investigate. Therefore, a value between 0.4 and 0.5 can be considered clinically optimal when looking at correlation-based connectivity. The static and dynamic network measures average path length and clustering coefficient/temporal correlation coefficient were calculated for each ROI for each subject. The mean and standard deviation of the network measures for each subject can be found in Figure 4.

### 3.3 | Predicting tic severity using LASSO regression

A predictor model for tic severity was created by applying linear regression with LASSO regularization to the network measures. This was preceded by a feature pre-selection step in which the Kendall's tau between each measure of each ROI and the YGTSS was computed, and those with a  $p$ -uncorrected  $<0.05$  were selected for the regression model. Gender and medication were used as additional binary covariates for the model. The leave one out validated LASSO regression model yielded a minimum mean squared error (MSE) of 0.53 at a lambda (positive regularization parameter) of 0.0140 (Figure 5a). The predicted YGTSS during each fold of the LOO validation showed a spearman correlation of 0.78 with the actual YGTSS. Figure 5b shows the correlation plot between the predicted YGTSS and the actual YGTSS. The coefficient of determination ( $R^2$ ), representing the goodness of fit, was found to be 0.43. In addition, we performed LOO-training + testing analyses, in which a LOO-validated model was created on 16 subjects and tested on 1 subject for each

different test subject. This, however, did not yield reliable results owing to the reduction in power. The results are available in Figure S2. The purpose of this study is to explore the regions that contribute to the predictor model creation, in order to better understand tic pathophysiology. The validation of this model needs to be performed in future studies on larger sample sizes.

### 3.4 | Feature space examination

Upon inspecting the feature space obtained by the model, five predictors were identified, all of which were dynamic sliding-window (dSW) network measures. There was no significant contribution by the static and dynamic ICA (dICA) networks. The temporal correlation coefficient (tCC) was the more relevant measure, with three out of eight identified features involving this measure. The other two features involved the average temporal path length (tAPL). Both binary predictors, gender, and medication, did not have any effect on the model. The specific regions and the corresponding features are explained in further detail in the following subsections.

#### 3.4.1 | The temporal correlation coefficient (tCC)

In the slow dynamic network (dSW network), the tCC of the left precentral gyrus (PreCG l), the right temporoparietal fusiform cortex (TOFus r) and the right caudate nucleus (Caudate r) were identified as predictors with Kendall's correlation coefficients of 0.36,  $-0.38$ ,  $-0.39$  and model weights of 0.56,  $-0.28$  and  $-0.24$ , respectively. As tics are typically motor in origin, it is no surprise that the primary motor cortex (i.e., PreCG l) appears as the predictor with the highest weight of 0.56 in the model. The temporal correlation coefficient indicates the stability of a node's subnetwork during the dynamic course of information processing. This means that over a broad temporal scale, the precentral gyrus typically switches communication channels, receiving from and sending information to different subnetworks over the course of time. Failure to do so results in the constant subnetwork participation observed in relation to tic severity. In contrast, the negative correlation of the tCC of the TOFus r and the Caudate r to the YGTSS indicates that an unstable subnetwork organization of these two regions may be related to tics.

#### 3.4.2 | The average temporal path length (tAPL)

In the slow dynamic network (dSW) the tAPL of the right supracalcarine cortex (SCC r) and the right frontal orbital cortex (FORb r) were identified as predictors with a Kendall's tau of 0.39 and 0.36 and model weights of  $-0.08$  and 0.31, respectively. The tAPL reflects how fast information is transferred between different subnetworks in time. A smaller temporal path length indicates that a node is well connected to other nodes across time and is thus active in dynamics, rapidly passing on information to other nodes. Consequently, our findings of positive correlation between the tAPL of FORb r and SCC r with the

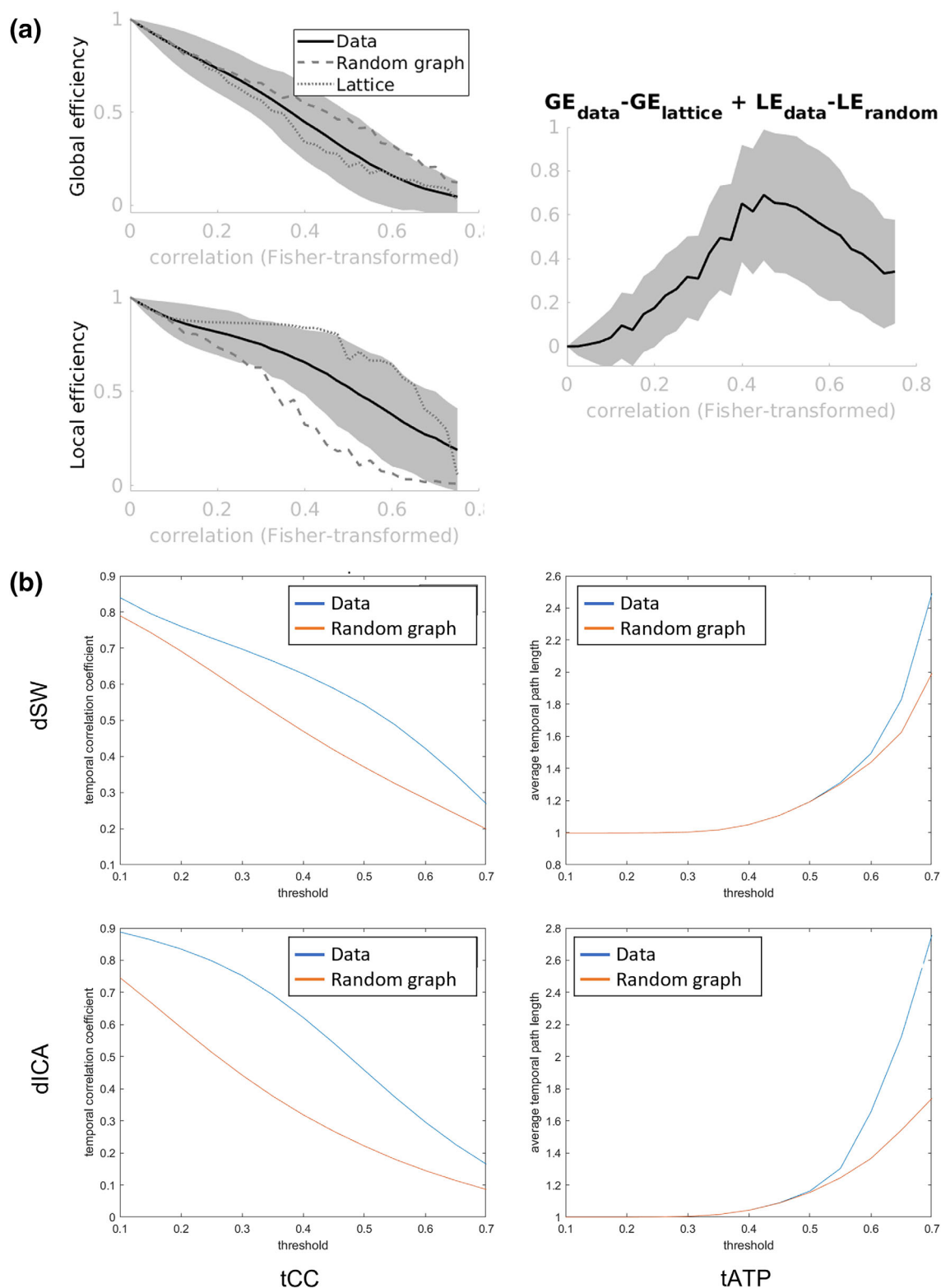


**FIGURE 3** Threshold determination for static and dynamic networks. (a) Variable threshold explorer in CONN v20. (b) As we can see, the separation between a random graph and lattice can be best observed between the threshold values 0.4–0.6. A value of 0.45 was chosen to retain as many connections as possible while maintaining optimal separation. (b) Variable threshold for the dSW and the dICA networks: Here too we see that at threshold values between 0.4 and 0.5, the average path length is  $>1$  but equally low for the random graph as our data and the temporal correlation coefficient is much higher than the corresponding random graph. Thus at these thresholds the network is small-world and to maintain consistency we chose a threshold 0.45.



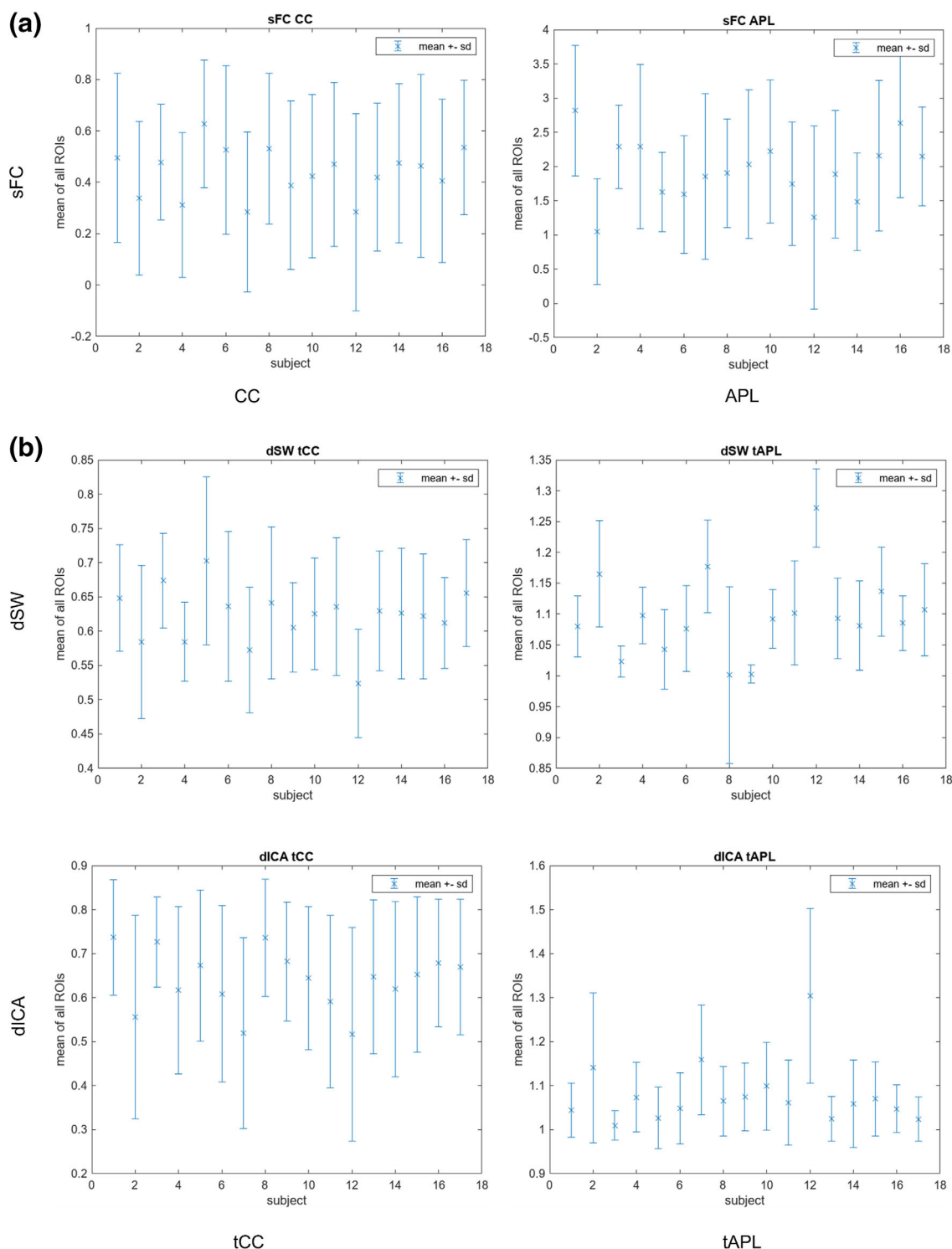


**FIGURE 4** Distribution of network measures. (a) mean and standard deviation of the static, average path length, and clustering coefficient/ (b) mean and standard deviation of the dynamic average path length, and temporal correlation coefficients of the dSW and the dICA networks.

YGTSS indicate selective connectedness and slow participation of the Forb r and the SCC r in time, contributing to tic severity.

The predictors of the dSW network with their respective Kendall's coefficients and weights visualized on a 3D brain volume can be seen in Figure 6.

## 4 | DISCUSSION

This study investigates the functional network correlates of tic severity in Tourette syndrome (TS) by using machine learning. Resting-state fMRI data from TS patients were preprocessed and quality controlled,

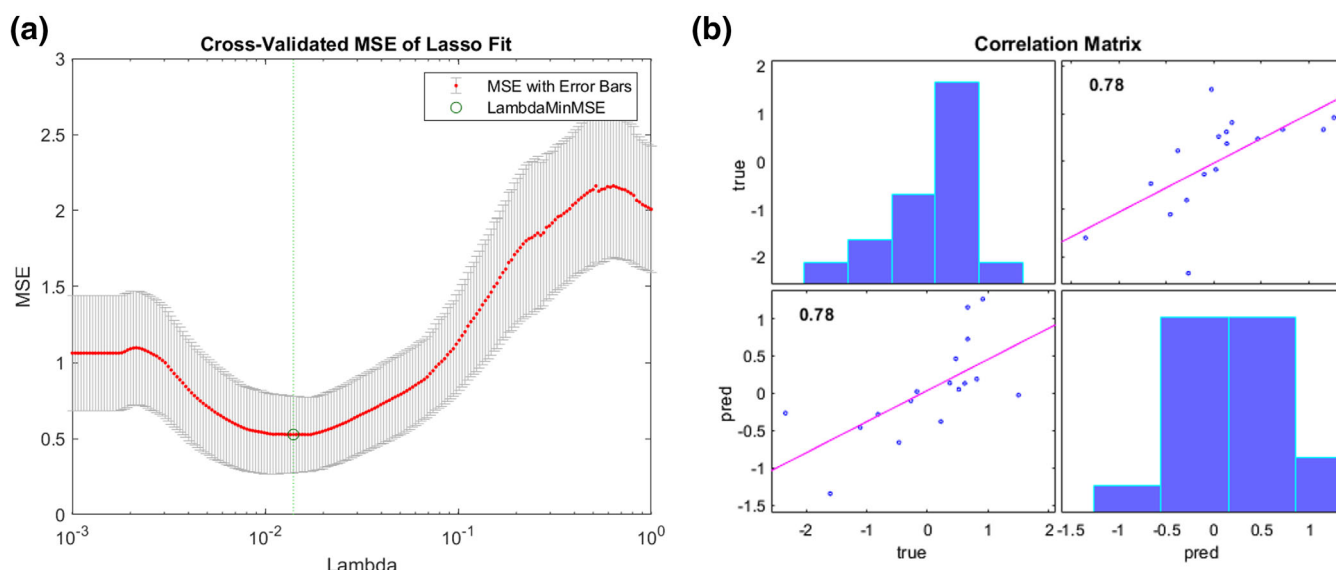


**FIGURE 5** Results of prediction model. (a) mean squared error (MSE) with error bars for LOO-validation of LASSO regression for different values of lambda. The value of lambda with the minimum MSE (shown by the green line) was chosen as the optimal model. (b) The correlation plot of the YGTSS predicted during LOO validation against the true YGTSS. Spearman's correlation is 0.78 and coefficient of determination is 0.4.

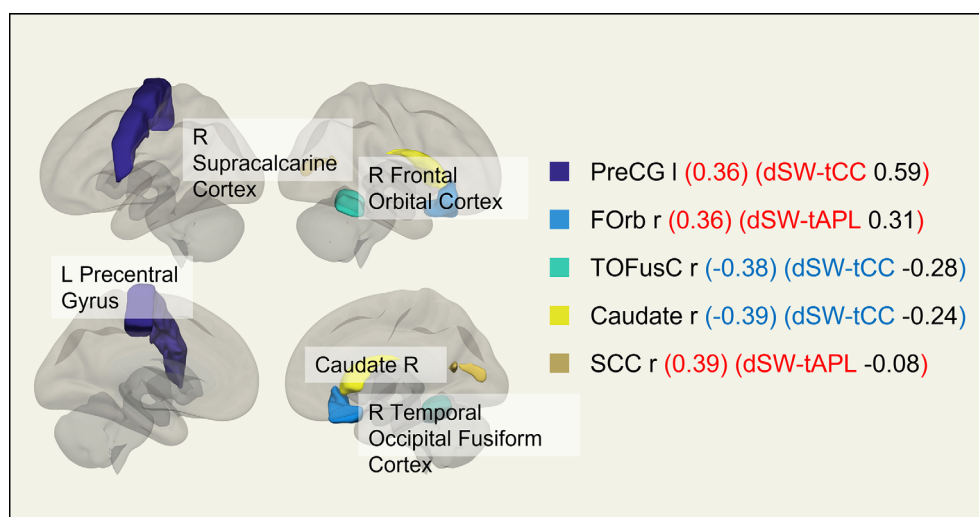


**FIGURE 6** Predictors of tic severity visualized. The features obtained by the LASSO regression model visualized on the brain surface. Red indicates a positive correlation with YGTSS, and blue indicates a negative correlation. The value of the Kendall's correlation coefficient is provided in the first parentheses, the network measure followed by its weight in the LASSO model is given in the second parentheses. All predictors belong to the dSW network.

and static and dynamic functional connectivity were calculated. Network theory was applied to evaluate brain communication strategies, and the topological metrics were included in a LASSO regression model against the Yale global tic severity scale (the YGTSS) to identify the network features which yield the best predictability.

All of the identified predictors belonged to the slow dynamic network (dSW network). Of these, the temporal correlation coefficient (tCC) was the most relevant metric with three significant regions, namely the left precentral gyrus (PreCG-I), the right temporo-occipital fusiform cortex (TOFusC-r) and the right caudate nucleus (Caudate r). The tCC of the PreCG-I was positively correlated with the YGTSS, indicating a consistency in the subnetwork of the PreCG-I during dynamic communication contributing to tic severity. Conversely, the tCC of the Caudate r and TOFusC-r were negatively correlated with

the YGTSS, indicating that changes in the subnetworks of these two regions during dynamic communication may be instrumental in tic severity. The preCG is the primary motor cortex that constantly communicates with other motor areas and subcortical brain regions to plan and execute movements (Alexander et al., 1986). Thus, the lack of network switching observed in dynamics indicates support for the lack of inhibition hypothesis (Jackson et al., 2015; Lerner et al., 2012). In normal brain functioning, spontaneous involuntary movements would be constantly balanced by inhibitory signals from other brain regions (observed as changing subnetworks in dynamics), and this failure of inhibitory control (observed as a constant subnetwork in dynamics) would lead to the sustained motor action observed in tics. Consistent activations in the pre-central gyrus have been reported 2 s and 1 s prior to tic onset and at tic onset (Neuner et al., 2014).

The TOFusC in our atlas corresponds to the subregion of the fusiform cortex specializing in face perception known as the fusiform face area (FFA) (Kanwisher & Yovel, 2006). It has been proposed that the FFA encodes abstract semantic information associated with faces, which is then later retrieved for social computations (Schultz et al., 2003). The social dimension of tics has been emphasized in literature (Albin, 2018), where it is proposed that TS is a disorder of the social decision-making network (SDM hypothesis). In this recent review article (Albin, 2018), Albin has shed light on the possibility of tics being distorted social signals, emphasizing the role of typical tic movements, such as head, neck, facial and hand movements, in non-verbal emotional communication (Ekman et al., 2013). The framework of this new hypothesis puts together different pieces of the complex puzzle, explaining the cardinal features of tic disorders, such as the nature of tics, sex disparity and natural course of the illness, together with the basal ganglia and amygdala abnormalities observed in imaging (Neuner et al., 2010; Ramkiran et al., 2019; Werner et al., 2010) and post-mortem studies (Albin, 2018). In this paper, Albin has further highlighted the three-fold role of the amygdala in social processing, that is, in social perception, affliction and aversion, proposing the idea that the performance of the amygdala in the social functioning networks centred around it is altered by task engagement and attentional loading, thus explaining the modulation of tics during task engagement. The involvement of the amygdala in social processing has also been highlighted by Adolphs and Spezio (2006). They have put forth the idea that the amygdala attentionally modulates the visual and somatosensory cortices, directing visuospatial attention to face gaze, thus guiding contextual social behaviour. This framework brings together the somatosensory, visual and attentional networks under the umbrella of the amygdala, making it the key background integrator of all these different networks. Thus, our findings relating to the TOFusC indicate that via the amygdala, attention is directed to abstract semantic information stored in relation to facial expressions of present or past experiences and which further motivates social behaviour. An unstable subnetwork organization of the TOFusC could be leading to misinterpreted social signals.

The caudate nucleus is a key region of the basal ganglia that has been shown to be implicated in tic disorders (Ramkiran et al., 2019). In a previous study (Ramkiran et al., 2019), we showed increased connectivity of the right caudate to several regions of the cortex and an increase in global efficiency in static networks as compared to healthy controls. Hyperkinetic disorders have been hypothesized to originate from a dysfunction of basal-ganglia-thalamo cortical circuits leading to hyperactivation of the motor cortex. Our current findings show that an unstable subnetwork organization of the Caudate *r* is responsible for tics.

The other two predictors of the dSW network were the average temporal path length (tAPL) of the right frontal orbital cortex (FORb *r*) and the right supracalcarine cortex (SCC *r*). The SCC, together with the occipital pole (OP), is the location of the primary visual cortex (Leuba & Kraftsik, 1994); however, preferential activation to face-targets over non-face visual stimuli have been reported in the SCC in an fMRI study (Dichter et al., 2009). This indicates its role in social processing and is in line with the SDM hypothesis of TS (Albin, 2018).

An unstable subnetwork organization, while playing a key role in information transfer, could indicate misinterpreted social signals (such as facial expressions) being transmitted to other subnetworks, driving inappropriate social behaviour, leading to tics (Albin, 2018).

The orbitofrontal cortex is a key region known to be involved in the control of motor planning, decision-making and working memory, through a basal ganglia loop. Reduced volumes with increasing tic severity have been reported previously (Müller-Vahl et al., 2009). The prefrontal areas comprising of the medial prefrontal and the orbitofrontal areas are considered highest in motor hierarchy. Two basal ganglia loops namely the dorsal prefrontal loop involving the dorsal caudate and ventroanterior thalamus, and the orbitofrontal circuit involving the ventromedial caudate and the dorsomedial pallidum, involve communication with prefrontal cortex (Weeks et al., 1996). It is proposed that the compulsion to tic originates in the orbitofrontal cortex which is why it is a key region implicated in OCD (Beucke et al., 2013). PET studies have shown increased perfusion in this area during symptom provocation (Weeks et al., 1996) in OCD patients. Our findings of slow and selective participation of FORb *r* in association to tic severity together with an unstable subnetwork organization of the Caudate *r* show strong evidence in favour of the orbitofrontal-basal ganglia circuit dysfunction.

There were no significant contributions of the dICA and the sFC network indicating that the most valuable information is provided by the slow dynamic communication. The faster dynamic and the static connectivity approaches fail to capture valuable information regarding tic pathophysiology. While it is understandable that the information captured by the sFC is incomplete as the temporal dimension is lacking, it is not entirely clear why the dICA approach fails too. One explanation could be that the faster dynamics are not really altered in tic disorders, and it is only the slower dynamics that lead to the symptomatology. Another possible explanation is that the dICA approach is not an accurate representation of the true dynamic connectivity as it is estimated based on group ICA. Since group ICA would ensure that only networks that are stable in the entire cohort are identified, and then further used to estimate the connectivity at the individual level, individual-level network instabilities could be potentially missed out. Further validation studies are needed to find out which one of the two is truly the case. In addition to the primary motor cortex and prefrontal cortex, our findings emphasize the role of several novel regions of the temporo-occipital cortex in TS. The temporo-occipital cortex is most well-known for its function as the visual cortex; however, more recently, its involvement in social processing (Adolphs & Spezio, 2006; Dichter et al., 2009) and psychiatric disorders, such as major depression (Liu et al., 2021), have come to light. These findings point to a new dimension of understanding that is in line with the emerging hypothesis of TS as a disorder of the social decision-making network (Albin, 2018). A proposed visual social processing network mediated by the amygdala (Adolphs & Spezio, 2006) involves communication between the regions obtained in our study through the amygdala. Thus, our network-based analysis approach helps in understanding how information is dynamically processed by each specific region engaged in this network in relation to tics in TS. It is interesting to

note that, while several studies have shown a direct implication of the amygdala in TS (Lerner et al., 2012; Neuner et al., 2010), our study demonstrates that the network properties of the amygdala itself are not direct predictors of tic severity, rather, the regions it communicates with in the social processing context are. This broadens our understanding on the roles played by other regions in the network in addition to the amygdala itself.

## 5 | CONCLUSION

This study investigated the predictability of tic severity in Tourette syndrome patients using machine learning on functional brain network static and dynamic topology. The machine learning approach used for this purpose was linear regression with Lasso regularization for predictor variable selection. Through this, several dynamic network measures and the corresponding key regions were identified as predictors of the Yale Global Tic Severity Scale. Network topological measures shed light on the communication strategies employed by the brain and our study highlights altered communication strategies in the primary motor cortex, and dysfunction in the amygdala-mediated social processing network and the basal-ganglia-thalamo-cortical network. These findings have opened up new dimensions of understanding for tic symptomatology.

## 6 | LIMITATIONS

The main limitation of this study is the small sample size owing to the difficulty in acquiring good quality data, free of motion artefacts arising due to the motor tics experienced by the patients. However, despite this, we observed convergence during leave one out validation, indicating the strength of our findings.

## ACKNOWLEDGEMENTS

We thank the German Tourette's Association for their support and travel funds and all participating Tourette's patients and their families for their cooperation, Ms. Claire Rick for her editorial input on writing the manuscript and the Medical Technical Assistants at the Forschungszentrum, Jülich for assistance with data acquisition. The data were acquired as part of a project funded by the Deutsche Forschungsgemeinschaft (DFG Nr. NE 1585/7-1). This study is part of the Dr. rer. medic thesis of Ms. Shukti Ramkiran. Open Access funding enabled and organized by Projekt DEAL.

## CONFLICT OF INTEREST STATEMENT

The authors declare no conflict of interest.

## DATA AVAILABILITY STATEMENT

All data are available for research purposes only upon request from the corresponding author. The data cannot be made publicly available due to ethical concerns regarding patient data.

## ORCID

Shukti Ramkiran  <https://orcid.org/0000-0001-8253-1873>

Ravichandran Rajkumar  <https://orcid.org/0000-0001-5875-5316>

N. Jon Shah  <https://orcid.org/0000-0002-8151-6169>

## REFERENCES

- Achard, S., & Bullmore, E. (2007). Efficiency and cost of economical brain functional networks. *PLoS Computational Biology*, 3, e17. <https://doi.org/10.1371/journal.pcbi.0030017>
- Adolphs, R., & Spezio, M. (2006). Role of the amygdala in processing visual social stimuli. In *Progress in brain research*. Elsevier.
- Albin, R. L. (2018). Tourette syndrome: A disorder of the social decision-making network. In *Brain*. Oxford Academic. <https://academic.oup.com/brain/article/141/2/332/4091478>
- Albin, R. L., & Mink, J. W. (2006). Recent advances in Tourette syndrome research. *Trends in Neurosciences*. <http://www.cell.com/article/S0166223606000026/fulltext>, 29, 175–182.
- Alexander, G. E., Delong, M. R., & Strick, P. L. (1986). Parallel Organization of functionally segregated circuits linking basal Ganglia and cortex. *Annual Review of Neuroscience*, 9, 357–381. <https://doi.org/10.1146/annurev.neuro.9.1.357>
- Alfonso Nieto-Castanon. (2020). *Handbook of functional connectivity Magnetic Resonance Imaging methods in CONN*. Hilbert Press. <https://doi.org/10.56441/hilbertpress.2207.6598>
- American Psychiatric Association. (2000). Diagnostic and statistical manual of mental disorders. Diagnostic and statistical manual of mental disorders (4th ed.), TR. [http://bvbr.bib-bvb.de:8991/F?func=service&doc\\_library=BVB01&local\\_base=BVB01&doc\\_number=025719079&line\\_number=0001&func\\_code=DB\\_RECORDS&service\\_type=MEDIA](http://bvbr.bib-bvb.de:8991/F?func=service&doc_library=BVB01&local_base=BVB01&doc_number=025719079&line_number=0001&func_code=DB_RECORDS&service_type=MEDIA)
- Ashburner, J., & Friston, K. J. (2005). Unified segmentation. *NeuroImage*, 26, 839–851.
- Bassett, D. S., & Bullmore, E. (2006). Small-world brain networks. *The Neuroscientist*, 12, 512–523. <https://doi.org/10.1177/1073858406293182>
- Bassett, D. S., Xia, C. H., & Satterthwaite, T. D. (2018). Understanding the emergence of neuropsychiatric disorders with network neuroscience. *Biological Psychiatry: Cognitive Neuroscience and Neuroimaging*, 3, 742–753.
- Beucke, J. C., Sepulcre, J., Talukdar, T., Linnman, C., Zschenderlein, K., Endrass, T., Kaufmann, C., & Kathmann, N. (2013). Abnormally high degree connectivity of the orbitofrontal cortex in obsessive-compulsive disorder. *JAMA Psychiatry*, 70, 619–629. <https://jamanetwork.com/journals/jamapsychiatry/fullarticle/1679420>
- Braun, U., Schäfer, A., Bassett, D. S., Rausch, F., Schweiger, J. I., Bilek, E., Erk, S., Romanczuk-Seiferth, N., Grimm, O., Geiger, L. S., Haddad, L., Otto, K., Mohnke, S., Heinz, A., Zink, M., Walter, H., Schwarz, E., Meyer-Lindenberg, A., & Tost, H. (2016). Dynamic brain network reconfiguration as a potential schizophrenia genetic risk mechanism modulated by NMDA receptor function. *Proceedings of the National Academy of Sciences of the United States of America*, 113, 12568–12573. <https://doi.org/10.1073/pnas.1608819113>
- Bullmore, E., & Sporns, O. (2009). Complex brain networks: Graph theoretical analysis of structural and functional systems. *Nature Reviews. Neuroscience*, 10, 186–198.
- Bullmore, E., & Sporns, O. (2012). The economy of brain network organization. *Nature Reviews. Neuroscience*, 13, 336–349.
- Cavanna, A. E., Servo, S., Monaco, F., & Robertson, M. M. (2009). The behavioral spectrum of Gilles de la Tourette syndrome. *The Journal of Neuropsychiatry and Clinical Neurosciences*, 21, 13–23. <https://doi.org/10.1176/jnp.2009.21.1.13>
- Damaraju, E., Allen, E. A., Belger, A., Ford, J. M., McEwen, S., Mathalon, D. H., Mueller, B. A., Pearson, G. D., Potkin, S. G., Preda, A., Turner, J. A., Vaidya, J. G., Van Erp, T. G., & Calhoun, V. D. (2014). Dynamic functional connectivity analysis reveals transient states of dysconnectivity in schizophrenia. *NeuroImage: Clinical*, 5, 298–308.



- Dichter, G. S., Felder, J. N., Bodfish, J. W., Sikich, L., & Belger, A. (2009). Mapping social target detection with functional magnetic resonance imaging. *Social Cognitive and Affective Neuroscience*, 4, 59–69.
- Ekman, P., Friesen, W. V., & Ellsworth, P. (2013). *Emotion in the human face: Guidelines for research and an integration of findings*. Pergamon Press. <https://doi.org/10.1016/C2013-0-02458-9>
- Fornito, A., Zalesky, A., & Bullmore, E. T. (2016). *Fundamentals of brain network analysis*. Elsevier. <http://www.sciencedirect.com/S0707/book/9780124079083/fundamentals-of-brain-network-analysis>
- Friston, K. J. (1994). Functional and effective connectivity in neuroimaging: A synthesis. *Human Brain Mapping*, 2, 56–78. <http://citeseerx.ist.psu.edu/viewdoc/download?doi=10.1.1.160.256&rep=rep1&type=pdf>
- Friston, K. J. (2011). Functional and effective connectivity: A review. *Brain Connectivity*, 1, 13–36.
- Friston, K. J., Holmes, A. P., Worsley, K. J., Poline, J.-P., Frith, C. D., & Frackowiak, R. S. J. (1994). Statistical parametric maps in functional imaging: A general linear approach. *Human Brain Mapping*, 2, 189–210. <https://doi.org/10.1002/hbm.460020402>
- Haas, M., Jakubovski, E., Fremer, C., Dietrich, A., Hoekstra, P. J., Jäger, B., & Müller-Vahl, K. R. (2021). Yale global tic severity scale (YGTS): Psychometric quality of the gold standard for tic assessment based on the large-scale EMTICS study. *Frontiers in Psychiatry*, 12, 98.
- Hutchison, R. M., Womelsdorf, T., Allen, E. A., Bandettini, P. A., Calhoun, V. D., Corbetta, M., Della Penna, S., Duyn, J. H., Glover, G. H., Gonzalez-Castillo, J., Handwerker, D. A., Keilholz, S., Kiviniemi, V., Leopold, D. A., de Pasquale, F., Sporns, O., Walter, M., & Chang, C. (2013). Dynamic functional connectivity: Promise, issues, and interpretations. *NeuroImage*, 80, 360–378.
- Jackson, G. M., Draper, A., Dyke, K., Pépés, S. E., & Jackson, S. R. (2015). Inhibition, disinhibition, and the control of action in Tourette syndrome. *Trends in Cognitive Sciences*, 19, 655–665.
- Kanwisher, N., & Yovel, G. (2006). The fusiform face area: A cortical region specialized for the perception of faces. *Philosophical Transactions of the Royal Society B*, 361, 2109–2128. <https://doi.org/10.1098/rstb.2006.1934>
- Latora, V., & Marchiori, M. (2001). Efficient behavior of small-world networks. *Physical Review Letters*, 87, 198701.
- Leckman, J. F., Riddle, M. A., Hardin, M. T., Ort, S. I., Swartz, K. L., Stevenson, J., & Cohen, D. J. (1989). The Yale global tic severity scale: Initial testing of a clinician-rated scale of tic severity. *Journal of the American Academy of Child and Adolescent Psychiatry*, 28, 566–573.
- Lerner, A., Bagic, A., Simmons, J. M., Mari, Z., Bonne, O., Xu, B., Kazuba, D., Herscovitch, P., Carson, R. E., Murphy, D. L., Drevets, W. C., & Hallett, M. (2012). Widespread abnormality of the  $\gamma$ -aminobutyric acid-ergic system in Tourette syndrome. *Brain*, 135, 1926–1936.
- Leuba, G., & Kraftsik, R. (1994). Changes in volume, surface estimate, three-dimensional shape and total number of neurons of the human primary visual cortex from midgestation until old age. *Anatomy and Embryology (Berlin)*, 190, 351–366. <https://doi.org/10.1007/BF00187293>
- Liu, D.-Y., Ju, X., Gao, Y., Han, J.-F., Li, Z., Hu, X.-W., Tan, Z.-L., Northoff, G., & Song, X. M. (2021). From molecular to behavior: Higher order occipital cortex in major depressive disorder. *Cerebral Cortex*, 32, 2129–2139. <https://doi.org/10.1093/cercor/bhab343/6382090>
- Mooneyham, B. W., Mrazek, M. D., Mrazek, A. J., Mrazek, K. L., Phillips, D. T., & Schooler, J. W. (2017). States of mind: Characterizing the neural bases of focus and mind-wandering through dynamic functional connectivity. *Journal of Cognitive Neuroscience*, 29, 495–506. [https://doi.org/10.1162/jocn\\_a\\_01066](https://doi.org/10.1162/jocn_a_01066)
- Müller-Vahl, K. R., Kaufmann, J., Grosskreutz, J., Dengler, R., Emrich, H. M., & Peschel, T. (2009). Prefrontal and anterior cingulate cortex abnormalities in Tourette syndrome: Evidence from voxel-based morphometry and magnetization transfer imaging. *BMC Neuroscience*, 10, 47.
- Neuner, I., Kellermann, T., Stöcker, T., Kircher, T., Habel, U., Shah, J. N., & Schneider, F. (2010). Amygdala hypersensitivity in response to emotional faces in Tourette's patients. *The World Journal of Biological Psychiatry*, 11, 858–872.
- Neuner, I., Wegener, P., Stoecker, T., Kircher, T., Schneider, F., & Shah, N. J. (2007). Development and implementation of an MR-compatible whole body video system. *Neuroscience Letters*, 420, 122–127.
- Neuner, I., Werner, C. J., Arrubla, J., Stöcker, T., Ehlen, C., Wegener, H. P., Schneider, F., & Shah, N. J. (2014). Imaging the where and when of tic generation and resting state networks in adult Tourette patients. *Frontiers in Human Neuroscience*, 8, 362. <https://doi.org/10.3389/fnhum.2014.00362/abstract>
- Ramkiran, S., Heidemeyer, L., Gaebler, A., Shah, N. J., & Neuner, I. (2019). Alterations in basal ganglia-cerebello-thalamo-cortical connectivity and whole brain functional network topology in Tourette's syndrome. *NeuroImage: Clinical*, 24, 101998.
- Robertson, M. M., Eapen, V., Singer, H. S., Martino, D., Scharf, J. M., Paschou, P., Roessner, V., Woods, D. W., Hariz, M., Mathews, C. A., Črnčec, R., & Leckman, J. F. (2017). Gilles de la Tourette syndrome. *Nature Reviews Disease Primers*, 3, 16097. <http://www.nature.com/articles/nrdp201697>
- Rogers, B. P., Morgan, V. L., Newton, A. T., & Gore, J. C. (2007). Assessing functional connectivity in the human brain by fMRI. *Magnetic Resonance Imaging*, 25, 1347–1357.
- Rubinov, M., & Sporns, O. (2010). Complex network measures of brain connectivity: Uses and interpretations. *NeuroImage*, 52, 1059–1069.
- Schultz, R. T., Grelotti, D. J., Klin, A., Kleinman, J., Van Der Gaag, C., Marois, R., & Skudlarski, P. (2003). The role of the fusiform face area in social cognition: Implications for the pathobiology of autism. *Philosophical Transactions of the Royal Society B*, 358, 415–427. <https://doi.org/10.1098/rstb.2002.1208>
- Sizemore, A. E., & Bassett, D. S. (2018). Dynamic graph metrics: Tutorial, toolbox, and tale. In *NeuroImage*. Academic Press Inc.
- Sporns, O. (2013). Structure and function of complex brain networks. *Dialogues in Clinical Neuroscience*, 15, 247–262.
- Storch, E. A., De Nadai, A. S., Lewin, A. B., McGuire, J. F., Jones, A. M., Mutch, P. J., Shytle, R. D., & Murphy, T. K. (2011). Defining treatment response in pediatric tic disorders: A signal detection analysis of the Yale global tic severity scale. *Journal of Child and Adolescent Psychopharmacology*, 21, 621–627.
- Tang, J., Scellato, S., Musolesi, M., Mascolo, C., & Latora, V. (2010). Small-world behavior in time-varying graphs. *Physical Review E: Statistical, Nonlinear, and Soft Matter Physics*, 81, 055101. <https://doi.org/10.1103/PhysRevE.81.055101>
- Vergara, V. M., Mayer, A. R., Kiehl, K. A., & Calhoun, V. D. (2018). Dynamic functional network connectivity discriminates mild traumatic brain injury through machine learning. *NeuroImage: Clinical*, 19, 30–37.
- Weeks, R. A., Turjanski, N., & Brooks, D. J. (1996). Tourette's syndrome: A disorder of cingulate and orbitofrontal function? *QJM*, 89, 401–408.
- Wen, H., Liu, Y., Rekik, I., Wang, S., Chen, Z., Zhang, J., Zhang, Y., Peng, Y., & He, H. (2017). Combining disrupted and discriminative topological properties of functional connectivity networks as neuroimaging biomarkers for accurate diagnosis of early Tourette syndrome children. *Molecular Neurobiology*, 55, 3251–3269. <https://doi.org/10.1007/s12035-017-0519-1>
- Wen, H., Liu, Y., Rekik, I., Wang, S., Zhang, J., Zhang, Y., Peng, Y., & He, H. (2017). Disrupted topological organization of structural networks revealed by probabilistic diffusion tractography in Tourette syndrome children. *Human Brain Mapping*, 38, 3988–4008.
- Werner, C. J., Stöcker, T., Kellermann, T., Wegener, H. P., Schneider, F., Shah, N. J., & Neuner, I. (2010). Altered amygdala functional connectivity in adult Tourette's syndrome. *European Archives of Psychiatry and Clinical Neuroscience*, 260, 99.

- Whitfield-Gabrieli, S., & Nieto-Castanon, A. (2012). Conn: A functional connectivity toolbox for correlated and Anticorrelated brain networks. *Brain Connectivity*, 2, 125–141.
- Worbe, Y., Malherbe, C., Hartmann, A., Péligrini-Issac, M., Messé, A., Vidailhet, M., Lehericy, S., & Benali, H. (2012). Functional immaturity of cortico-basal ganglia networks in Gilles de la Tourette syndrome. *Brain*, 135, 1937–1946.
- Xie, Y., Xu, Z., Xia, M., Liu, J., Shou, X., Cui, Z., Liao, X., & He, Y. (2022). Alterations in connectome dynamics in autism Spectrum disorder: A harmonized mega- and meta-analysis study using the autism brain imaging data exchange dataset. *Biological Psychiatry*, 91, 945–955.
- Yin, W., Li, T., Mucha, P. J., Cohen, J. R., Zhu, H., Zhu, Z., & Lin, W. (2022). Altered neural flexibility in children with attention-deficit/hyperactivity disorder. *Molecular Psychiatry*, 27(11), 4673–4679 <https://www.nature.com/articles/s41380-022-01706-4>

## SUPPORTING INFORMATION

Additional supporting information can be found online in the Supporting Information section at the end of this article.

**How to cite this article:** Ramkiran, S., Veselinović, T., Dammers, J., Gaebler, A. J., Rajkumar, R., Shah, N. J., & Neuner, I. (2023). How brain networks tic: Predicting tic severity through rs-fMRI dynamics in Tourette syndrome. *Human Brain Mapping*, 44(11), 4225–4238. <https://doi.org/10.1002/hbm.26341>